Supporting Information

Rational design of monodispersed Au@Pt core-shell nanostructure with excellent peroxidase-mimicking activity for colorimetric detection of Cr(VI)

Taohong Zhou,[a] Jin Lin,[a] Fengmei Jin,[b] Yanxing Yao,[b] Zhihao Li,*[b] and Lihua Wang*[a,b]

[a]Key Laboratory of Detection Technology of Focus Chemical Hazards in Animal-derived Food for State Market Regulation, Wuhan, 430070, China

[b]Wuhan Academy of Agricultural Sciences, Wuhan, 430072, China

Email: zhh_li@whu.edu.cn, wanglihua19850116@126.com

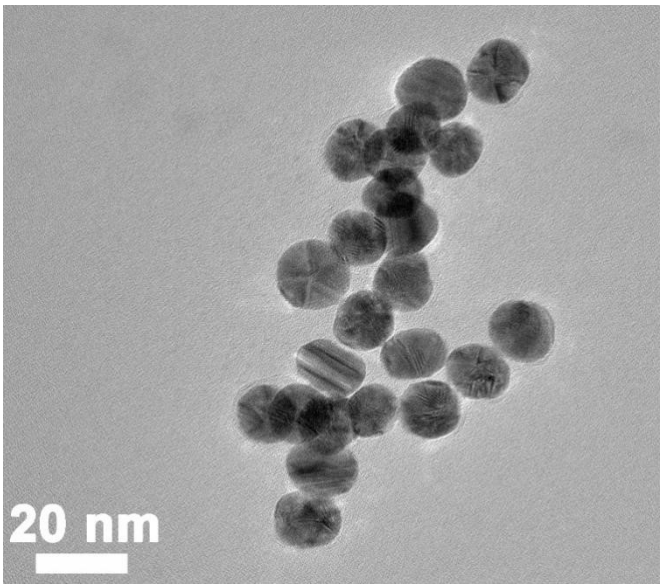

Figure S1. TEM images of 15 nm Au nanoparticles.

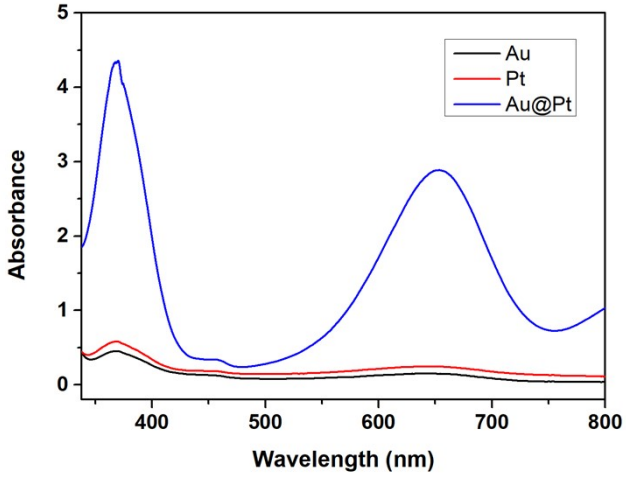

Figure S2. UV-Vis spectra of the reactions systems catalyzed by Au nanoparticles, Pt nanoparticles, and Au@Pt nanoparticles, respectively.

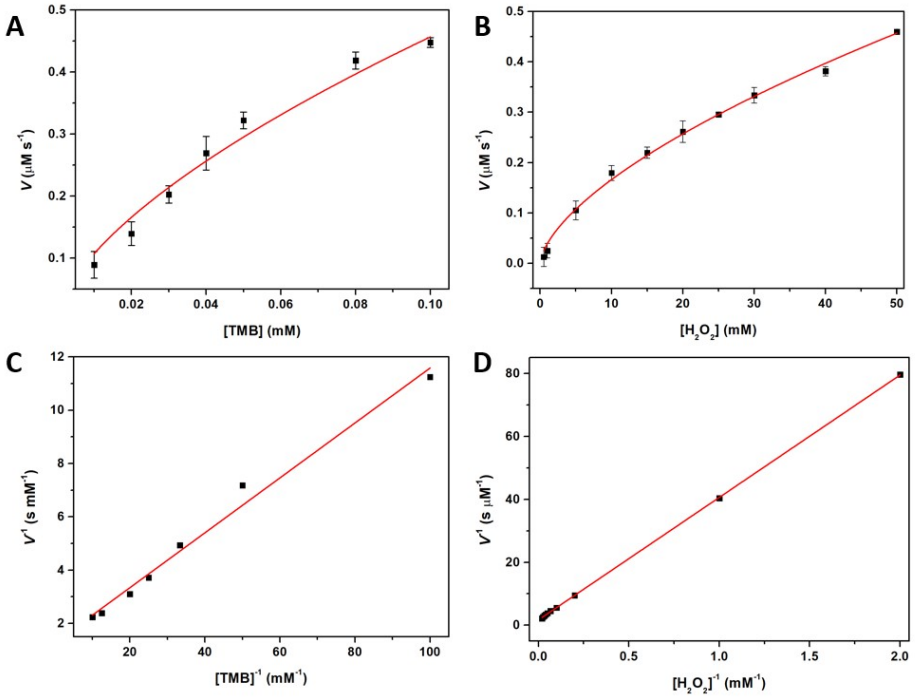

Figure S3. The Michaelis-Menten curves of Au@Pt nanoparticles towards (A) TMB and (B) H_2O_2. The Lineweaver-Burk plots of Au@Pt nanoparticles towards (C) TMB and (D) H_2O_2.

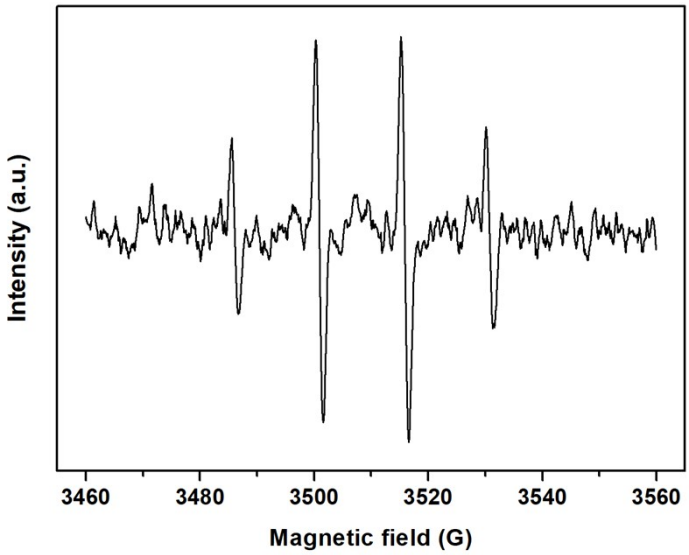

Figure S4. ESR spectrum of Au@Pt nanoparticles.

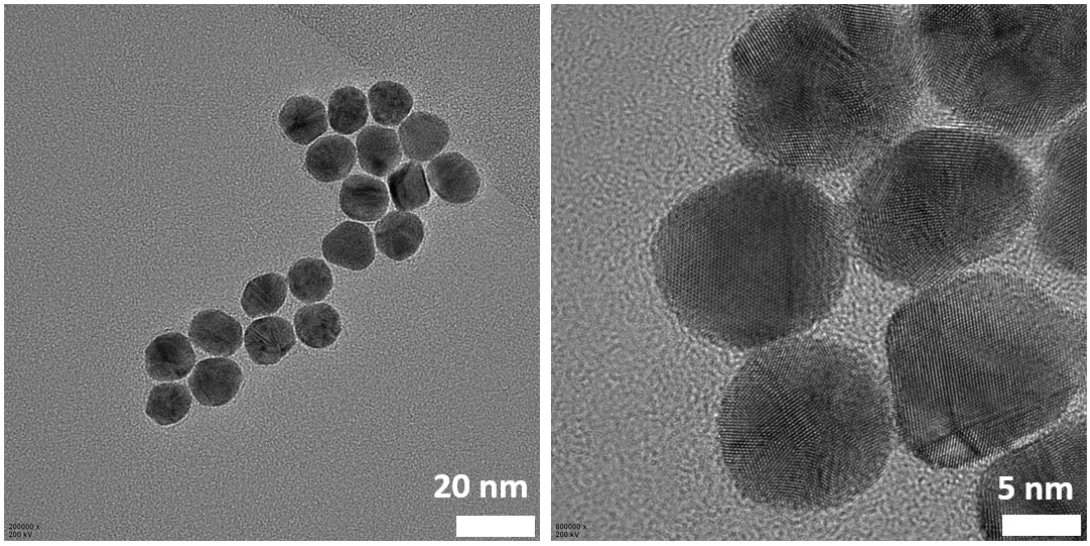

Figure S5. TEM images of Au@Pt nanoparticles after addition of Cr(VI).

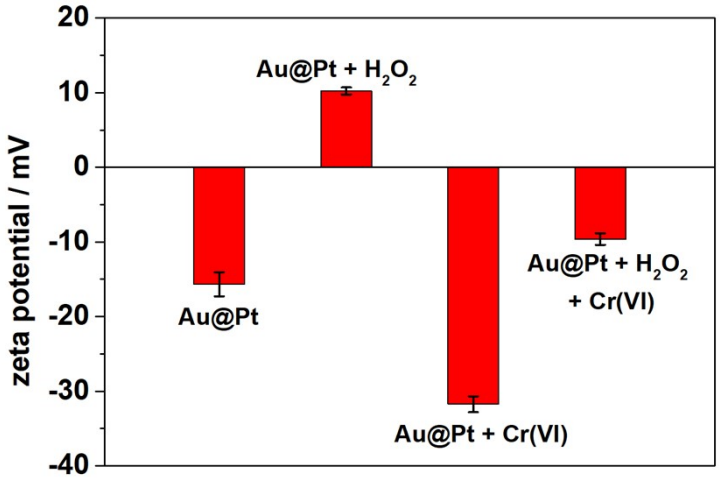

Figure S6. Zeta potentials of the system containing Au@Pt, Au@Pt + H_2O_2, Au@Pt + Cr(VI), and Au@Pt + H_2O_2 + Cr(VI).

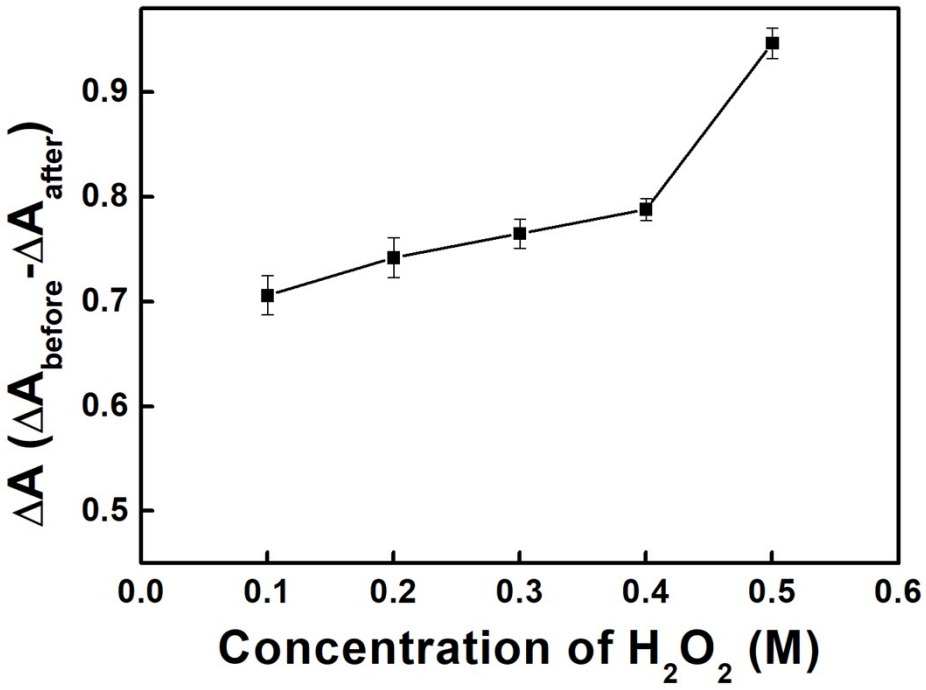

Figure S7. Effect of H_2O_2 concentration on the ΔA response of Au@Pt nanozyme-based assays.

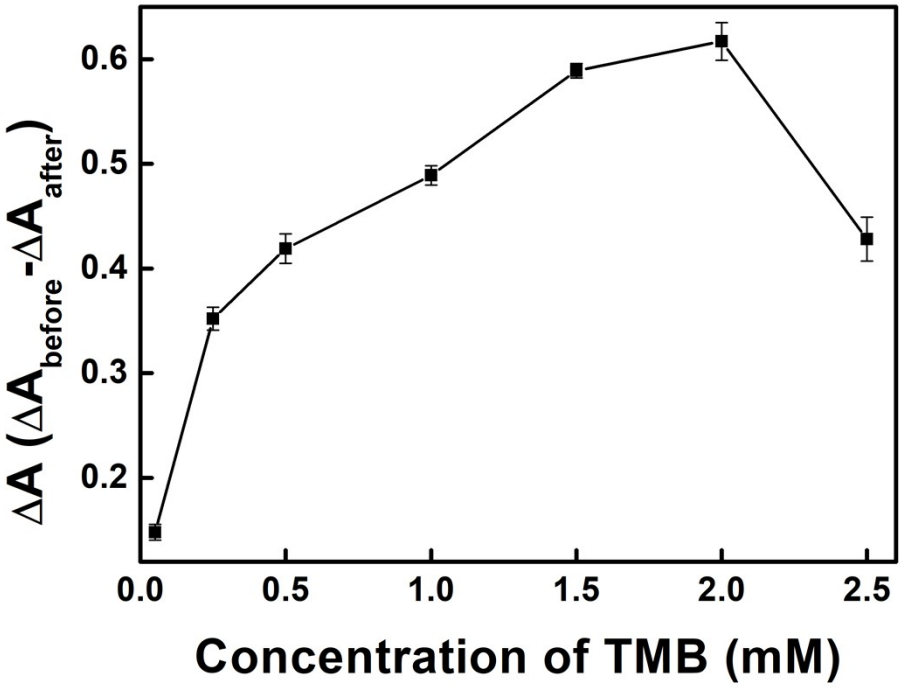

Figure S8. Effect of TMB concentration on the ΔA response of Au@Pt nanozyme-based assays.

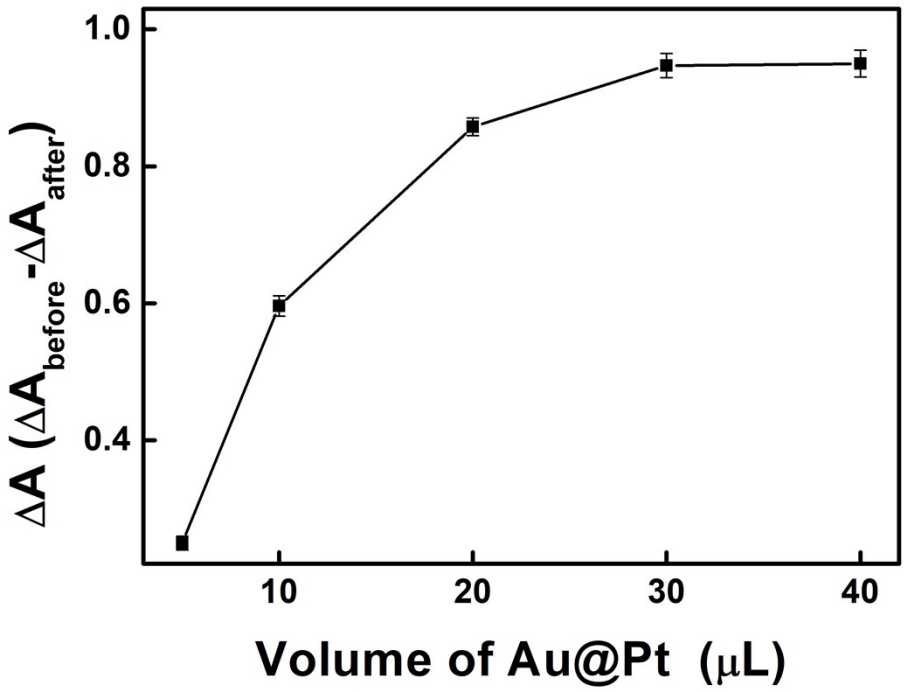

Figure S9. Effect of volume of Au@Pt on the ΔA response of Au@Pt nanozyme-based assays.

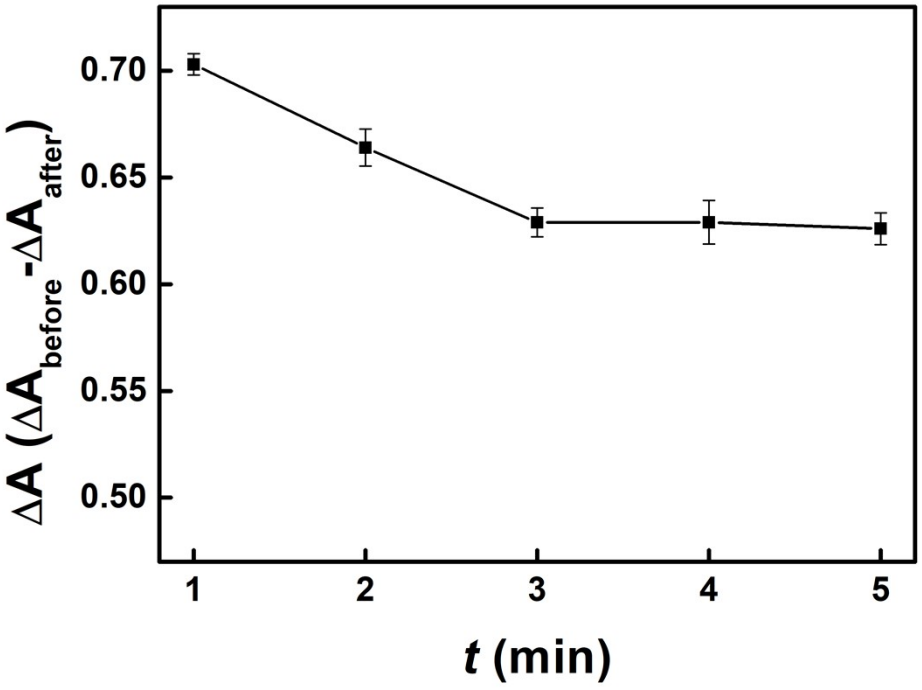

Figure S10. Effect of oxidation reaction time (reaction time before Cr(VI) addition) on the ΔA response of Au@Pt nanozyme-based assays.

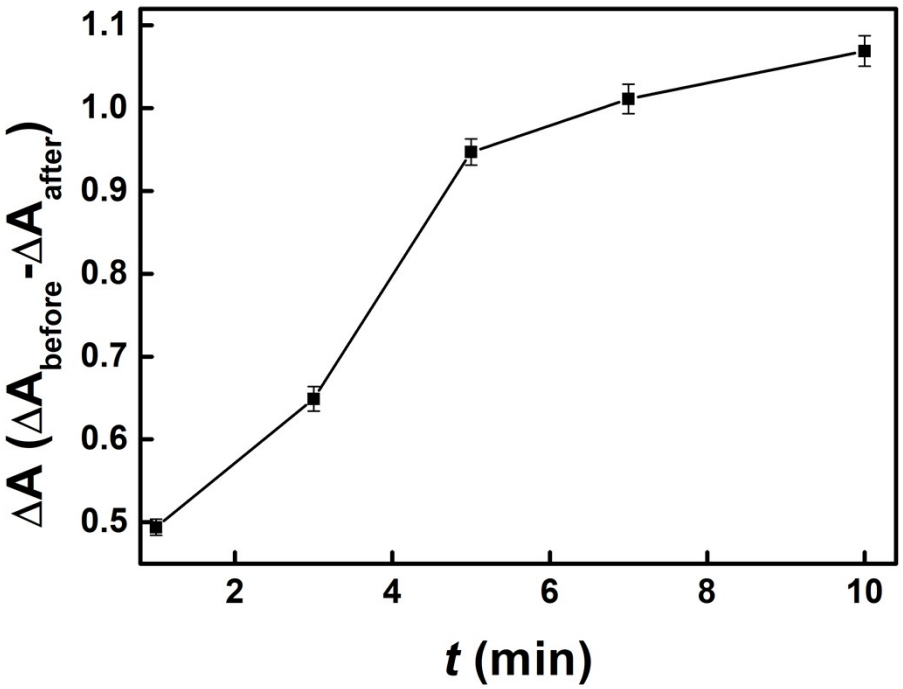

Figure S11. Effect of reaction time after Cr(VI) addition on the ΔA response of Au@Pt nanozyme-based assays.

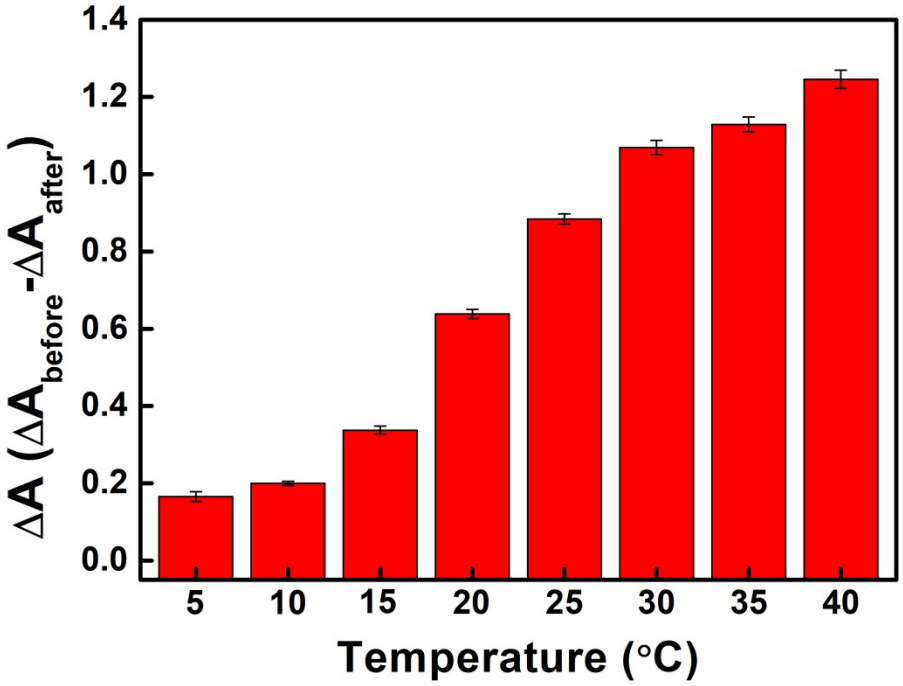

Figure S12. Effect of reaction temperature on the ΔA response of Au@Pt nanozyme-based assays.

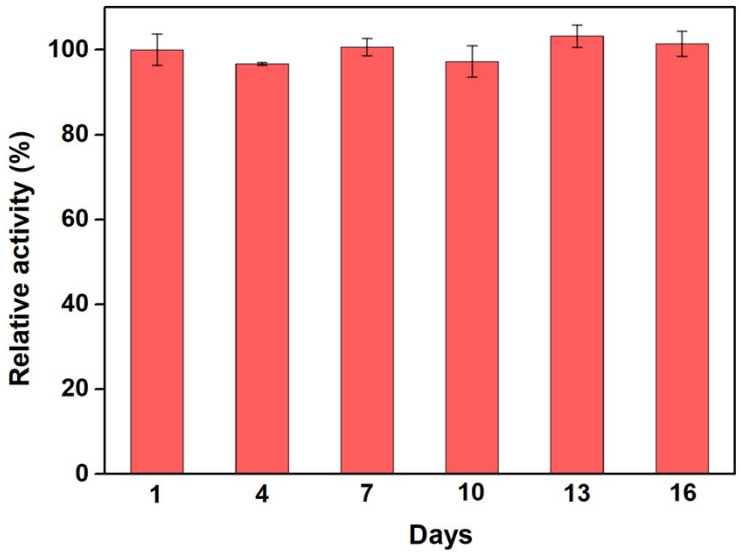

Figure S13. Relative activity of Au@Pt-based sensor after storage for different days.

Table S1. Comparison of the kinetic parameters of various catalysts toward the oxidation of TMB by H_2O_2.

Catalyst	K_m		V_{max} (μM s^{-1})		Reference
	TMB	H_2O_2	TMB	H_2O_2	
Fe_3O_4@MOF@Pt	0.49	125	0.22	0.22	1
UsAuNPs/2D MOF	0.14	0.05	0.052	0.13	2
Pd-Ir cubes	0.13	340	0.065	0.051	3
BSA-stabilized Pt NPs	0.119	41.8	0.21	0.17	4
Pt-HMCNs	0.124	0.086	0.15	0.12	5
PtNPs/Cu-TCPP(Fe)	0.044	37.67	0.16	0.46	6
Fe_3O_4@MoS_2@Pt	0.86	23.04	0.18	0.13	7
HRP	0.817	0.63	0.053	0.094	1
Au@Pt nanoparticles	0.08	22.74	0.78	0.58	This work

Table S2. Comparison of the analytical performance between the Au@Pt nanozyme-based assays with other reported nanozyme-based assays.

Material	Method	Linear range	LOD (μM)	Reference
rGO/PEI/Au nanohybrids	Colorimetric	5 nM-10 μM	2.14×10^{-3} μM	8
Cal-CS/PEG/Ag	Colorimetric	0.09-20 μM	0.079 μM	9
Fe_3O_4	Colorimetric	0-500 μM	0.03465 μM	10
Cu-PyC MOF	Colorimetric	0.5-50 μM	0.051 μM	11
PEI-AgNCs	Colorimetric	5-100 μM	1.10 μM	12
Polyoxometalate-based crystalline materials	Electrochemical	2-2.61 mM	0.174 μM	13
Ag NPs	Surface-enhanced	2 ppb-50 ppm	0.72 ppb	14

	Raman spectroscopy			
CuS-frGO	Fluorescence	0-200 nM	26.6 nM	15
AuNCs	Fluorescence	10 ppb-10 ppm	7.2 μM	16
Au@Pt nanoparticles	Colorimetric	5 ppb-2.0 ppm	0.5 ppb (9.8 nM)	This work

References

[1] Rui Chen, Xirui Chen, Yaofeng Zhou, Tong Lin, Yuankui Leng, Xiaolin Huang, Yonghua Xiong. "Three-in-One" multifunctional nanohybrids with colorimetric magnetic catalytic activities to enhance immunochromatographic diagnosis. *ACS Nano* **2022**, *16*, 3351−3361.

[2] Huanyu Yang, Zhiping Sun, Xinguang Qin, Hongyuan Wu, Haizhi Zhang, Gang Liu. Ultrasmall Au nanoparticles modified 2D metalloporphyrinic metal-organic framework nanosheets with high peroxidase-like activity for colorimetric detection of organophosphorus pesticides. *Food Chem.* **2022**, *376*, 131906.

[3] Xiaohu Xia, Jingtuo Zhang, Ning Lu, Moon J. Kim, Kushal Ghale, Ye Xu, Erin McKenzie, Jiabin Liu, Haihang Ye. Pd-Ir core-shell nanocubes: A type of highly efficient and versatile peroxidase mimic. *ACS Nano*, **2015**, *9*, 9994−10004.

[4] Wei Li, Bin Chen, Haixiang Zhang, Yanhua Sun, Jun Wang, Jinli Zhang, Yan Fu. BSA-stabilized Pt nanozyme for peroxidase mimetics and its application on colorimetric detection of mercury(II) ions. *Biosens. Bioelectron.* **2015**, *66*, 251−258.

[5] Haitao Chen, Chenyi Yuan, Xuanyu Yang, Xiaowei Cheng, Ahmed Elzatahry, Abdulaziz Alghamdi, Jiacan Su, Xing He, Yonghui Deng. Hollow mesoporous carbon nanospheres loaded with Pt nanoparticles for colorimetric detection of ascorbic acid and glucose. *ACS Appl. Nano Mater.* **2020**, *3*, 4586−4598.

[6] Huayun Chen, Qiming Qiu, Sumaira Sharif, Shengna Ying, Yixian Wang, Yibin Ying. Solution-phase synthesis of platinum nanoparticle-decorated metal-organic framework hybrid nanomaterials as biomimetic nanoenzymes for biosensing applications. *ACS Appl. Mater. Interfaces* **2018**, *10*, 24108−24115.

[7] Meimei Xu, Shuai Zhao, Chenglong Lin, Yanyan Li, Weida Zhang, Yusi Peng, Rui Xiao, Zhengren Huang, Yong Yang. Dual-mode lateral flow immunoassay based on "Pompon Mum"-like Fe_3O_4@MoS_2@Pt nanotags for sensitvie detection of viral pathogens. *ACS Appl. Mater. Interfaces* **2024**, *16*, 11172−11184.

[8] Teng Zhang, Shouting Zhang, Jia Liu, Jing Li, Xiaoquan Lu. Efficient visual chemosensor for hexavalent chromium via a controlled strategy for signal amplification in water. *Anal. Chem.* **2020**, *92*, 3426−3433.

[9] Meili Liu, Shouting Zhang, Yingsha Wang, Jia Liu, Wenping Hu, Xiaoquan Lu. Hexavalent chromium as a smart switch for peroxidase-like activity regulation via the surface electronic redistribution of silver nanoparticles anchored on carbon spheres. *Anal. Chem.* **2022**, *94*, 1669–1677.

[10] Melisew Tadele Alula, Mildred Lesang Madingwane. Colorimetric quantification of chromium(VI) ions based on oxidoreductase-like activity of Fe_3O_4. *Sens. Actuators B. Chem.* **2020**, *324*, 128726.

[11] Sivasankar Kulandaivel, Wen-Chi Lo, Chia-Her Lin, Yi-Chun Yeh. Cu-PyC MOF with

oxidoreductase-like catalytic activity boosting colorimetric detection of Cr(VI) on paper. *Anal. Chim. Acta* **2022**, *1227*, 340335.
[12] Qiangsheng Xue, Xin Li, Yinxian Peng, Peng Liu, Hongbing Peng, Xiangheng Niu. Polyethylenimine-stabilized silver nanoclusters act as an oxidoreductase mimic for colorimetric determination of chromium(VI). *Microchim. Acta*, **2020**, *187*, 263.
[13] Xing Xin, Na Hu, Yuanyuan Ma, Yali Wang, Lin Hou, Heng Zhang, Zhangang Han. Polyoxometalate-based crystalline materials as a highly sensitive electrochemical sensor for detecting trace Cr(VI). *Dalton Trans*. **2020**, *49*, 4570−4577.
[14] Cuijuan Wang, Ming Shang, Haiyan Wei, Mengping Zhang, Wei Zou, Xiao Meng, Wenwen Chen, Hua Shao, Yongchao Lai. Specific and sensitive on-site detection of Cr(VI) by surface-enhanced Raman spectroscopy. *Sens. Actuators B. Chem.* **2021**, *346*, 130594.
[15] Priyakshree Borthakur, Manash R. Das, Sabine Szunerits, Rabah Boukherroub. CuS decorated functionalized reduced graphene oxide: A dual responsive nanozyme for selective detection and photoreduction of Cr(VI) in an aqueous medium. *ACS Sustainable Chem. Eng.* **2019**, *7*, 16131−16143.
[16] Feiyan Liu, Xuandi Lai, Shengliang Zhao, Zhiyang Lu, Peigang Han, Liqiong Chen. A simple and feasible fluorescent approach for rapid detection of hexavalent chromium based on gold nanoclusters. *Food Chem.* **2023**, *402*, 134251.